

LASER-PLASMA ACCELERATION OF ELECTRONS DOI: 10.1070/QE2016v046n01ABEH015944

Precession dynamics of the relativistic electron spin in laser-plasma acceleration

D.V. Pugacheva, N.E. Andreev

Abstract. **A model is developed to study the precession dynamics of the relativistic electron spin in a laser-plasma accelerator versus the initial energy of the electron and its injection phase. Optimal parameters providing minimum depolarisation of the electron in the acceleration process are determined.**

Keywords: *laser-plasma acceleration, spin precession, electron polarisation dynamics.*

1. Introduction

Spin represents a fundamental property of particles on a par with the mass and charge and significantly affects the interaction cross section of the particle bunches in high-energy physics experiments [1]. The interaction cross section depends on the polarisation defined by the average spin of the particles comprising a bunch. Currently, the studies being conducted on modern accelerators employ polarised bunches of particles, thus allowing, for example, testing the accuracy of a standard model [1, 2]. Some accelerators have been purposely modernised, while others are initially designed with allowance for the use of polarised particle sources. Spin dynamics in accelerators [3] has been investigated and methods for controlling the degree and polarisation direction have been developed [4].

Maximal acceleration gradients that can be achieved in conventional accelerators, and the increase in which directly affects the accelerator size and cost, are limited by the breakdown threshold of the waveguide wall material. In the 1970s, an alternative way of electron acceleration was proposed, based on the use of the so-called wake field generated in plasma under the action of short and intense laser pulses. The acceleration gradients in this method are several orders of magnitude higher compared to the field gradients in traditional accelerators [5]. A successful experimental demonstration of the high (100 GeV m^{-1}) [6] gradient has given an impetus to further development of this field of research. Different scientific teams attain increasingly greater particle energies by improving laser technology and waveguide structures. To date, the highest result constitutes 4 GeV [7], while theory shows that the energies exceeding those obtained in conventional high-frequency linear accelerators are quite achievable. Therefore, a study that will enable us to determine the variation range of the electron bunch polarisation during the laser-plasma acceleration and to understand the factors it depends on, is very urgent.

The aim of this work is to study the dynamics of the electron polarisation in the laser-plasma accelerator. For this purpose, a model and a set of computer programmes have been developed for numerical evaluation of the spin precession of the electron during its acceleration in the wake-field wave generated by a laser pulse in the plasma channel. The precession dynamics of a single electron versus the injection phase and initial energy is analysed. The parameters that ensure minimal deviation of the electron spin from its initial value during the acceleration process are derived. The results of a self-consistent numerical simulation are compared with some theoretical estimates of acceleration in constant fields.

2. Basic equations

When a laser pulse interacts with low-density plasma, electrons turn out shifted relative to ions under the high-frequency pressure action. The thus emerging electron density fluctuations give rise to a wake-field wave which may accelerate electrons to a high energy. In this paper we consider the acceleration of electrons in a wake field formed by the passage of a short high-intensity laser pulse along the z axis of a cylindrically symmetric plasma channel with increasing radial plasma concentration. Numerical simulation of the nonlinear wake-field waves is performed using the LAPLAC code [8] based on the solution of hydrodynamic equations describing the dynamics of a cold relativistic ideal electron liquid, jointly with Maxwell's equations [9–11]:

$$\frac{\partial n}{\partial t} + \nabla(n\boldsymbol{v}) = 0, \tag{1}$$

$$\frac{\partial \boldsymbol{p}}{\partial t} = e\boldsymbol{E} - mc^2\nabla\gamma_p, \tag{2}$$

$$\frac{\partial \boldsymbol{E}}{\partial t} = -4\pi ne\boldsymbol{v} - \frac{c^2}{e}\nabla\times\nabla\times\boldsymbol{p}, \tag{3}$$

$$\gamma_p = \sqrt{1 + \frac{p^2}{m^2c^2} + \frac{|a|^2}{2}}, \quad \boldsymbol{v} = \frac{\boldsymbol{p}}{m\gamma_p}, \tag{4}$$

and the equation that determines the evolution of the normalised complex envelope of the laser pulse $a = eE_L/(mc\omega)$ [8, 12]:

$$\left(\frac{2i\omega}{c^2}\frac{\partial}{\partial t} + 2ik\frac{\partial}{\partial z} - \Delta_\perp\right)a = \frac{\omega_{p0}}{c^2}\left(\frac{n}{N_0\gamma_p} - 1\right)a, \tag{5}$$

D.V.Pugacheva, N.E. Andreev Joint Institute for High Temperatures, Russian Academy of Sciences, ul. Izhorskaya 13, Bld. 2, 125412 Moscow, Russia; e-mail: sedyakina.d@gmail.com

Received 08 October 2015; revision received 17 November 2015
Kvantovaya Elektronika **46** (1) 88–93 (2016)
Translated by M.A. Monastyrskiy

where c is the speed of light; n, $\boldsymbol{p}$ and $\boldsymbol{v}$ are the concentration, specific momentum and speed of electrons in the plasma; e and m are the charge and mass of electrons; N_0 is the initial electron density on the plasma channel axis; $\omega_{p0} = \sqrt{4\pi e^2 N_0/m}$ is the plasma frequency; ω and $k = \omega/c$ are the frequency and wave number of laser radiation; $\boldsymbol{E}$ is the electric field in plasma, which slowly varies on the scales ω^{-1} and k^{-1}; and $\Delta_\perp$ is the transverse part of the Laplace operator. The complex amplitude E_L of the laser field is associated with the high-frequency electric field $\tilde{\boldsymbol{E}}$ of the laser pulse by the relation

$$\tilde{\boldsymbol{E}} = \boldsymbol{e}_L \mathrm{Re}\{E_L \exp[-\mathrm{i}(\omega t - kz)]\}, \tag{6}$$

where $\boldsymbol{e}_L$ is the laser pulse polarisation vector.

Using the dimensionless variables

$$\xi = k_{p0}(z - ct),\ \zeta = k_{p0} z,\ \boldsymbol{\rho} = k_{p0}\boldsymbol{r}_\perp, \tag{7}$$

where $k_{p0} = \omega_{p0}/c$, we can re-write equation (5) with regard to cylindrical symmetry in the form [8, 12]

$$\left[2\mathrm{i}\frac{\partial}{\partial\zeta} + \frac{k_{p0}}{k}\left(\Delta_{\perp\rho} + 2\frac{\partial^2}{\partial\zeta\partial\xi}\right)\right]a = \frac{k_{p0}\nu}{k\gamma_p}a, \tag{8}$$

where $\nu = n/N_0$; and

$$\Delta_{\perp\rho} = \frac{1}{\rho}\frac{\partial}{\partial\rho}\rho\frac{\partial}{\partial\rho}.$$

The nonlinear relativistic plasma response ν/γ_p can be expressed through the scalar function (potential) $\Phi = \gamma_p - p_z/(mc)$ [8, 12]:

$$\frac{\nu}{\gamma_p} = \frac{\nu_0 + \Delta_\perp\Phi}{1 + \Phi}, \tag{9}$$

where $\nu_0 = n_0/N_0$; $n_0 = n_0(\rho,\zeta)$ is the initial distribution of electrons; and the wake-field potential Φ is normalised to mc^2/e. In the quasi-static approximation [13], in the case of a 'wide' (compared to the length $1/k_{p0}$) laser pulse, system (1)–(4) gives an equation for the potential [12]

$$\left[(\Delta_{\perp\rho} - \nu_0)\frac{\partial^2}{\partial\xi^2} - \frac{\partial\ln\nu_0}{\partial\rho}\frac{\partial^3}{\partial\rho\partial\xi^2} + \nu_0\Delta_{\perp\rho}\right]\Phi$$
$$- \frac{\nu_0^2}{2}\left[1 - \frac{1 + |a|^2/2}{(1+\Phi)^2}\right] = \nu_0\Delta_{\perp\rho}\frac{|a|^2}{4}. \tag{10}$$

In the dimensionless variables, the motion equations for electrons take the form [8, 14]

$$\frac{\mathrm{d}q_z}{\mathrm{d}\tau} = F_z(\xi,\rho), \tag{11}$$

$$\frac{\mathrm{d}\boldsymbol{q}_\perp}{\mathrm{d}\tau} = \boldsymbol{F}_r(\xi,\boldsymbol{\rho}), \tag{12}$$

$$\frac{\mathrm{d}\xi}{\mathrm{d}\tau} = \frac{q_z}{\gamma} - 1, \tag{13}$$

$$\frac{\mathrm{d}\boldsymbol{\rho}}{\mathrm{d}\tau} = \frac{\boldsymbol{q}_\perp}{\gamma}, \tag{14}$$

where the forces acting on a relativistic electron moving along the z axis with a speed close to the speed of light can be expressed in terms of the potential Φ [12]:

$$F_z = E_z = \frac{\partial\Phi}{\partial\xi},\quad F_r = E_r - B_\phi = \frac{\partial\Phi}{\partial\rho}. \tag{15}$$

Here, the components of electric ($\boldsymbol{E}$) and magnetic ($\boldsymbol{B}$) fields are normalised to $mc\omega_{p0}/e$; $\boldsymbol{F}_r = \{F_x, F_y\} = F_r\{\cos\phi, \sin\phi\}$; q_z and $\boldsymbol{q}_\perp = \{q_x, q_y\}$ are the longitudinal and transverse components of the dimensionless electron pulse $\boldsymbol{q} = \boldsymbol{p}_e/(mc)$; $\phi = \arctan(y/x)$ is the angle characterising the position of the electron in the plane xy; $\tau = \omega_{p0}t$ is the dimensionless time; and $\gamma = \sqrt{1 + q_z^2 + q_\perp^2}$ is the relativistic electron factor.

The equation describing the spin precession of a relativistic electron,

$$\frac{\mathrm{d}\boldsymbol{s}}{\mathrm{d}t} = -\frac{e}{mc}\left[\left(a_m + \frac{1}{\gamma}\right)\boldsymbol{B} - \frac{a_m\gamma}{\gamma+1}(\boldsymbol{\beta}\boldsymbol{B})\boldsymbol{\beta}\right.$$
$$\left. - \left(a_m + \frac{1}{\gamma+1}\right)\boldsymbol{\beta}\times\boldsymbol{E}\right]\times\boldsymbol{s}, \tag{16}$$

was obtained in 1959 by V. Bargmann, L. Michel and V. Telegdi [15], and is referred to in the literature as the Thomas–BMT equation. In this equation $a_m \approx 0.0011614$ is the anomalous magnetic moment of the electron, and $\boldsymbol{\beta} = \boldsymbol{v}_e/c$ is the normalised electron velocity. It should be emphasised that the spin $\boldsymbol{s}$ in (16) is defined in the particle's rest frame, while all other values, including the fields $\boldsymbol{E}$ and $\boldsymbol{B}$, are given in the laboratory frame. Furthermore, it is assumed that the spin does not affect the particle trajectory.

On the basis of equation (16), using the facts that the magnetic field in a cylindrically symmetric plasma channel is azimuthal, $\boldsymbol{B} = B_\phi\boldsymbol{e}_\phi$, the electric field only contains the longitudinal and transverse components, and $\boldsymbol{E} = E_r\boldsymbol{e}_r + E_z\boldsymbol{e}_z$, let us formulate a system of differential equations in the Cartesian coordinate system in terms of the dimensionless variables (7), describing the spin precession of an electron, the speed of which along the plasma channel axis is close to the speed of light, while its transverse velocity component is small compared to the speed of light:

$$\frac{\mathrm{d}s_x}{\mathrm{d}\tau} = s_z\left(a_m + \frac{1}{\gamma}\right)F_r\cos\phi, \tag{17}$$

$$\frac{\mathrm{d}s_y}{\mathrm{d}\tau} = s_z\left(a_m + \frac{1}{\gamma}\right)F_r\sin\phi, \tag{18}$$

$$\frac{\mathrm{d}s_z}{\mathrm{d}\tau} = -\left(a_m + \frac{1}{\gamma}\right)F_r(s_x\cos\phi + s_y\sin\phi), \tag{19}$$

where with allowance for $\beta_z \approx 1$ and $\gamma = 1/\sqrt{1-\beta^2} \gg 1$, it is assumed that $a_m + 1/(\gamma+1) \approx a_m + 1/\gamma$. Thus, relations (8), (10)–(15) and (17)–(19) represent a closed system of equations describing the acceleration of polarised electrons in the wake-field wave generated by a laser pulse in the plasma channel.

3. Spin precession dynamics of relativistic electrons

In this work, the electron dynamics and spin precession have been simulated by means of numerical solution of equations

(11)–(14) and (17)–(19) in the dimensionless coordinates ζ, ξ, ρ:

$$\frac{dq_z}{d\zeta} = \frac{1}{\beta_z}\frac{\partial \Phi}{\partial \xi}, \quad \frac{dq_x}{d\zeta} = \frac{1}{\beta_z}\frac{\partial \Phi}{\partial \rho}\cos\phi,$$
$$\frac{dq_y}{d\zeta} = \frac{1}{\beta_z}\frac{\partial \Phi}{\partial \rho}\sin\phi, \tag{20}$$

$$\frac{d\xi}{d\zeta} = 1 - \frac{1}{\beta_z}, \quad \frac{dx}{d\zeta} = \frac{q_x}{q_z}, \quad \frac{dy}{d\zeta} = \frac{q_y}{q_z}, \tag{21}$$

$$\frac{ds_x}{d\zeta} = \frac{s_z}{\beta_z}\left(a_m + \frac{1}{\gamma}\right)\frac{\partial \Phi}{\partial \rho}\cos\phi, \tag{22}$$

$$\frac{ds_y}{d\zeta} = \frac{s_z}{\beta_z}\left(a_m + \frac{1}{\gamma}\right)\frac{\partial \Phi}{\partial \rho}\sin\phi, \tag{23}$$

$$\frac{ds_z}{d\zeta} = -\frac{1}{\beta_z}\left(a_m + \frac{1}{\gamma}\right)\frac{\partial \Phi}{\partial \rho}(s_x\cos\phi + s_y\sin\phi), \tag{24}$$

where $\beta_z = q_z/\gamma$. The forces acting on an accelerated electron are calculated by means of numerical solution of the self-consistent problem represented by equations (8), (10) and (15) in the LAPLACE code [8]; in the case of constant fields, these forces are assumed to take the prescribed constant values.

3.1. Simulation results in constant fields

To obtain an approximate analytical description of the spin precession of an accelerated electron and to test the numerical implementation of the model, we consider the motion of relativistic electrons under the action of the constant accelerating field $\boldsymbol{E}_{ac}$ and the linear focusing force F_r:

$$F_z = E_{ac}, \quad F_r = \alpha|\boldsymbol{x}_\perp|, \tag{25}$$

where the vector $\boldsymbol{x}_\perp = \{x, y\}$ defining the electron position in the plane perpendicular to the direction of its acceleration is normalised to k_{p0}. Under assumption that the transverse component of the electron velocity is much smaller than the speed of light, the gamma-factor (i.e. the energy) of accelerated electron increases in time linearly: $\gamma = \gamma_0 + E_{ac}\tau$, where $\gamma_0 = \gamma(\tau = 0)$, and the equation of its oscillation relative to the transverse coordinate $\boldsymbol{x}_\perp$ has a form [16]

$$(\gamma_0 + E_{ac}\tau)\ddot{\boldsymbol{x}}_\perp(\tau) + \gamma_0\dot{\boldsymbol{x}}_\perp(\tau) + \alpha\boldsymbol{x}_\perp(\tau) = 0. \tag{26}$$

In the approximation $\sqrt{|\alpha|\gamma_0}/E_{ac} \gg 1$ [17] this equation can be solved analytically:

$$\boldsymbol{x}_\perp(\tau) = \boldsymbol{x}_{\perp 0}\left[\frac{\gamma_0}{\gamma(\tau)}\right]^{1/4}\cos\left[\frac{2\sqrt{|\alpha|}}{E_{ac}}(\sqrt{\gamma} - \sqrt{\gamma_0})\right]$$
$$+ \boldsymbol{q}_{\perp 0}\frac{1}{(\alpha^2\gamma\gamma_0)^{1/4}}\sin\left[\frac{2\sqrt{|\alpha|}}{E_{ac}}(\sqrt{\gamma} - \sqrt{\gamma_0})\right], \tag{27}$$

where $\boldsymbol{x}_{\perp 0} = \{x_0, y_0\}$ and $\boldsymbol{q}_{\perp 0}$ are the initial position and momentum of the electron, respectively.

The system of equations (17)–(19) describing the spin precession of a test particle in the cylindrical coordinate system attached to the electron's initial position appear as [17]:

$$\frac{ds_r}{d\tau} = s_z\left(a_m + \frac{1}{\gamma}\right)F_r' + s_\phi\dot{\phi}, \tag{28}$$

$$\frac{ds_z}{d\tau} = -s_r\left(a_m + \frac{1}{\gamma}\right)F_r', \tag{29}$$

$$\frac{ds_\phi}{d\tau} = -s_r\dot{\phi}, \tag{30}$$

where $\dot{\phi} \equiv d\phi/d\tau$; $F_r' = F_r(|x_0|\cos\phi + |y_0|\sin\phi)/\sqrt{x_0^2 + y_0^2}$; the spin $\boldsymbol{s}$ is normalised to its absolute value so that any spin projection may range from –1 to 1; and $s_r^2 + s_\phi^2 + s_z^2 = 1$. If the condition $|\boldsymbol{x}_{\perp 0}|\sqrt{|\alpha|\gamma_0} \gg |\boldsymbol{q}_{\perp 0}|$ is fulfilled, the electron trajectory can be considered virtually planar; therefore, $ds_\phi/d\tau \ll 1$ and the spin component s_ϕ is preserved. In this case, the expression following from (28)–(30) and describing a variation of the spin s_z-component can be represented as

$$s_z(\tau) = \sqrt{1 - s_{\phi 0}^2}\sin\left[-\int_0^t\left(a_m + \frac{1}{\gamma}\right)F_r'\,dt + \arctan\left(\frac{s_{z0}}{s_{r0}}\right)\right]. \tag{31}$$

By using a small parameter

$$\frac{3E_{ac}}{4a_m\sqrt{\alpha}(\gamma\gamma_0^5)^{1/4}} \ll 1 \tag{32}$$

calculation of the integral in (31) provides an analytical formula for the dynamics of the spin component $s_z(\tau)$ [17]

$$s_z(\gamma(\tau)) = \sqrt{1 - s_{\phi 0}^2}\sin\left[-r_0\Omega(\tau) + \arctan\left(\frac{s_{z0}}{s_{r0}}\right)\right], \tag{33}$$

where $r_0 = (x_0|x_0| + y_0|y_0|)/\sqrt{x_0^2 + y_0^2}$; and

$$\Omega(\tau) = (1 + a_m\gamma)\left(\frac{\alpha^2\gamma_0}{\gamma^3}\right)^{1/4}\sin\left[\frac{2\sqrt{|\alpha|}}{E_{ac}}(\sqrt{\gamma} - \sqrt{\gamma_0})\right].$$

In the case of the pre-defined constant accelerating and focusing fields, condition (32) is fulfilled the better the greater are the values of γ and γ_0. To evaluate analytically the precession at moderate γ_0 and γ, when parameter (32) becomes of the order of unity, it is necessary to take into account the additional terms in the expansion of integral (31), which leads to the expression

$$s_z(\gamma(\tau)) = \sqrt{1 - s_{\phi 0}^2}\sin\left[\Lambda - \frac{3r_0E_{ac}}{4\gamma_0}\times\right.$$
$$\left.\times\left(1 - \left(\frac{\gamma_0}{\gamma}\right)^{5/4}\cos\left[\frac{2\sqrt{|\alpha|}}{E_{ac}}(\sqrt{\gamma} - \sqrt{\gamma_0})\right]\right) + \arctan\left(\frac{s_{z0}}{s_{r0}}\right)\right], \tag{34}$$

where

$$\Lambda = -r_0(1 + a_m\gamma)\left(\frac{\alpha^2\gamma_0}{\gamma^3}\right)^{1/4}\sin\left[\frac{2\sqrt{|\alpha|}}{E_{ac}}(\sqrt{\gamma} - \sqrt{\gamma_0})\right].$$

To test the numerical implementation of model (20)–(24), we have conducted relevant calculations for the accelerating field $E_{ac} = 0.47492$ and the linear focusing force with $\alpha = -0.07544$. The initial value of the electron position $\boldsymbol{x}_{\perp 0} = \{0.15, 0.2\}$ and its spin in the Cartesian coordinates $\{\boldsymbol{s}_0 = 0.27941, 0.33456, 0.9\}$ correspond to the value $s_{r0} = 0.1$ of the radial component of spin in the cylindrical coordinate system attached to the initial position of the electron. Figure 1 shows the results of

numerical solution of equations (20)–(24) for an electron with $\gamma_0 = 2\times10^4$ in comparison with the values obtained from formulas (33) and (34) with the same parameters. It is seen that, for given initial conditions, the simulation results virtually coincide with the analytical values, which allows us to conclude that the numerical implementation of equations (20)–(24) is correct.

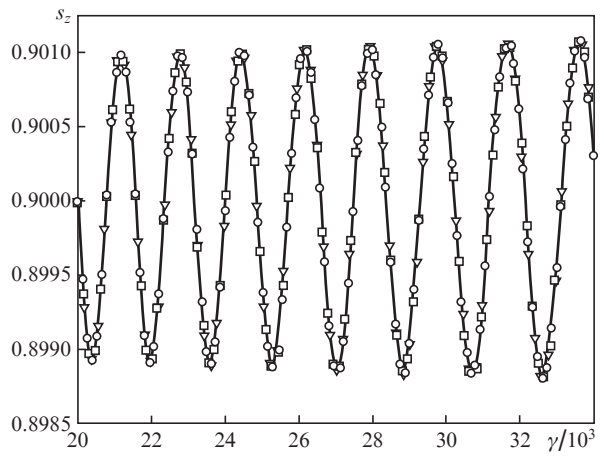

Figure 1. Precession dynamics of the s_z-component of the spin of an electron moving under the action of forces (25) at $E_{ac} = 0.47492$, $\alpha = -0.07544$, $\gamma_0 = 2\times10^4$ vs. the electron gamma factor $\gamma \simeq \sqrt{1+q_z^2}$: the results of numerical solution of equations (20)–(24) (△) and calculation according to formulas (33) (○) and (34) (□) with the same parameters.

It should be noted that formula (34) transforms into (33) in the limit of large γ_0 (Fig.1). Figure 2 illustrates the difference between the values provided by these analytical formulas for an electron with $\gamma_0 = 132$. We may see that the simulation results with these parameters are in good agreement with the results of calculation by means of formula (34).

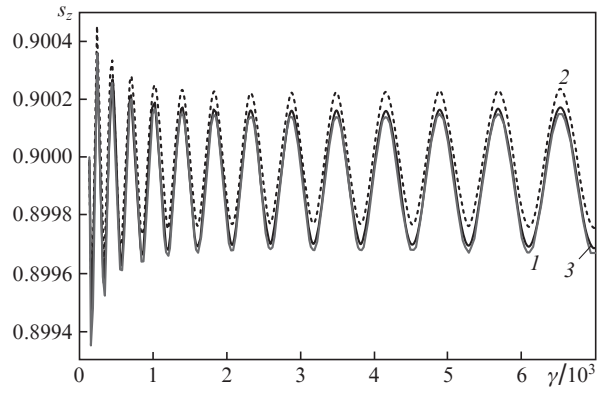

Figure 2. Same as in Fig. 1, but for $\gamma_0 = 132$: the results of numerical solution of the equations (20)–(24) (*1*) and calculation according to formulas (33) (*2*) and (34) (*3*).

3.2. Results of self-consistent numerical simulation of electron spin precession in laser-plasma acceleration

We study the dynamics of the spin polarisation for an electron being accelerated in the wake-field wave generated by a laser pulse propagating along the z axis of a cylindrically symmetric plasma channel with a parabolic electron density profile in the plane xy perpendicular to the z axis [10]:

$$n_0 = N_0\left(1 + \frac{r^2}{R_{ch}^2}\right), \tag{35}$$

where R_{ch} is the typical radial dimension of the channel; and $N_0 = 10^{17}$ cm^{-3}, which corresponds to the wave number $k_{p0} = 0.0595$ μm^{-1} of the plasma wave. Use of the plasma channel allows preventing the diffraction broadening of the laser pulse and ensures its propagation at a distance being much greater than the Rayleigh length. The laser pulse evolution and wake-field generation have been described by means of numerical solution of equations (8) and (10) with the LAPLAC code [8] for a channel with $R_{ch} = 305.1$ μm ($k_{p0}R_{ch} \simeq 18 > \rho_m$, where $\rho_m = {}^1\!/_2(k_{p0}r_L)^2 \simeq 14$ is the channel radius correlated with the momentum in linear approximation) and a Gaussian pulse possessing at the channel entrance an envelope

$$a(\xi,\rho,\zeta=0) = a_0\exp\left[-\frac{\rho^2}{\rho_L^2} - \left(\frac{\xi-\xi_{L0}}{\xi_L}\right)^2\right] \tag{36}$$

with $a_0 = 1.414$, $\rho_L = 5.303$, $\xi_L = 10$ and $\xi_{L0} = 7$, which corresponds to the following dimensional characteristics of the laser pulse: the focal spot radius of $r_L = \rho_L k_{p0}^{-1} = 89.13$ μm, the length of $t_L = \xi_L\omega_{p0}^{-1} = 56$ fs, the intensity of $I_L = 4.28\times10^{18}$ W cm^{-2}, and the power of 534 TW at a laser wavelength of $\lambda = 0.8$ μm.

The depolarisation of the electron has been studied versus its initial energy ε_0, and the phase position $\boldsymbol{x}_{\perp0}$ at the injection time moment. We consider two limiting cases: 1) $\varepsilon_0 = \varepsilon_{res}$, where $\varepsilon_{res} = \gamma_{ph}mc^2$ is the resonant energy at which the electron velocity at the time of injection coincides with the phase velocity V_{ph} of the wake wave: $\gamma_{ph} = 1/\sqrt{1 - V_{ph}^2/c^2} \simeq \omega/\omega_{p0}$, and 2) $\varepsilon_0 \gg \varepsilon_{res}$. The acceleration length L_{ac} constitutes 50.42 cm for all cases ($L_{ac} < L_{ph}$, where $L_{ph} = 2\pi\gamma_{ph}^2k_{p0}^{-1} \simeq 184$ cm is the length of electron dephasing relative to the wake wave). Figures 3a and 3b demonstrate the laser pulse envelope, the potential Φ and the accelerating force F_z at the start ($z = 0$) and the end ($z = 50.42$ cm) of acceleration; the position of the electron with $\xi_0 = 3.2$ at the injection time moment is schematically indicated. Figure 4 shows the contour lines of the focusing force F_r in the plane $\rho\xi$ at the start and end of acceleration, which illustrates a change in the forces acting on the electron in the acceleration process. As can be seen from Figs 3 and 4, the forces acting on the accelerated electron are nonconstant as a consequence of both the nonlinear evolution of the laser pulse during its propagation in the plasma channel and the displacement of the electron relative to the wake wave.

We consider the effect of variability of the forces acting on the accelerated electron and its spin precession in the case of injection of an electron with the resonance energy $\gamma_0 = \gamma_{ph} = 132$ at point $\xi_0 = 3.2$ at a distance of $r_0 = 0.25$ from the z axis, with the values of $\boldsymbol{x}_{\perp0} = \{0.15, 0.2\}$ and $\phi_0 = 0{,}927$, which corresponds to the position of the electron at the initial spin orientation $\boldsymbol{s} = \{0.27941, -33456, 0.9\}$. In this case we may compare the precession of the component s_z specified by the analytical formula (34) for an average value of the forces acting on the particle during the acceleration process with the results of a full-scale simulation with allowance for the laser pulse dynamics and the generated wake field. Averaging of

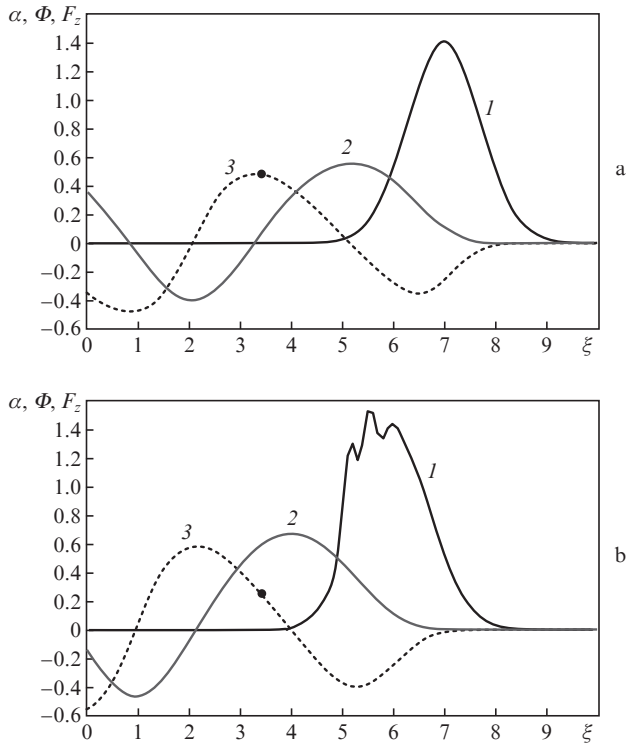

Figure 3. Dimensionless distributions of the laser pulse envelope a (*1*), wake-wave potential Φ (*2*) and accelerating force F_z (*3*) on the plasma channel axis vs. the ξ value at the start ($z = 0$) (a) and end ($z = 50.42$ cm) (b) of the electron acceleration. Black dot corresponds to the position of the electron with $\xi_0 = 3.2$.

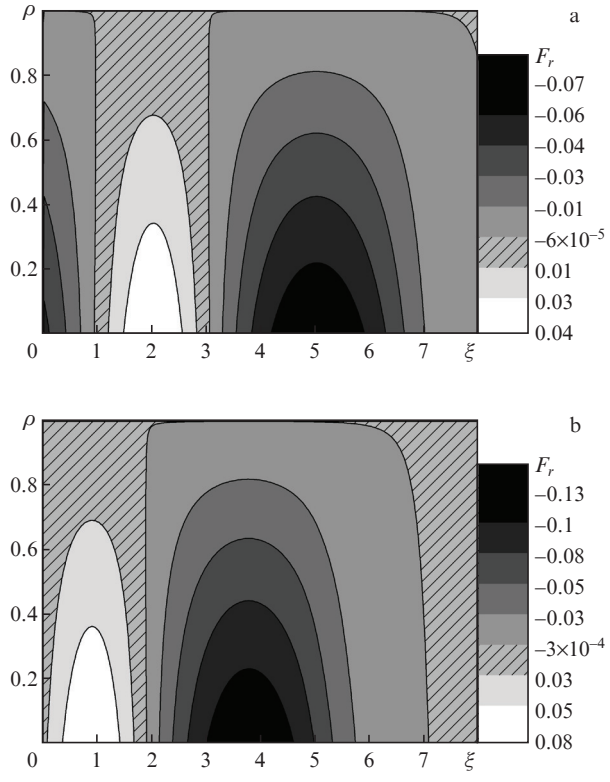

Figure 4. 2D distribution of the dimensionless focusing force $F_r(\rho,\xi)$ at the start (a) and end (b) of the electron acceleration.

the forces acting on the electron having the coordinates $r_{\perp e}, z_e$ has been performed throughout the acceleration length $L_{ac} = 50.42$ cm. For the accelerating force we have

$$F_z^{av} = \frac{1}{L_{ac}} \int_{z=0}^{L_{ac}} F_z(r_{\perp e}, z_e)\, dz;$$

for the focusing force $F_r^{av} = \alpha^{av} \rho_\perp$, where α^{av} is the averaged α obtained by means of linear approximation of the force $F_r(r_\perp, z_e)$ near the channel axis. The data in Fig. 5 demonstrate that the precession dynamics of the longitudinal component of the electron spin in static fields [formula (34)] is significantly different from the spin precession evolution in the dynamic fields of a wake wave [equations (8) and (10), (15), (20)–(24)]; this points to a need for numerical calculations in the studies on depolarisation of electrons in the laser-plasma acceleration.

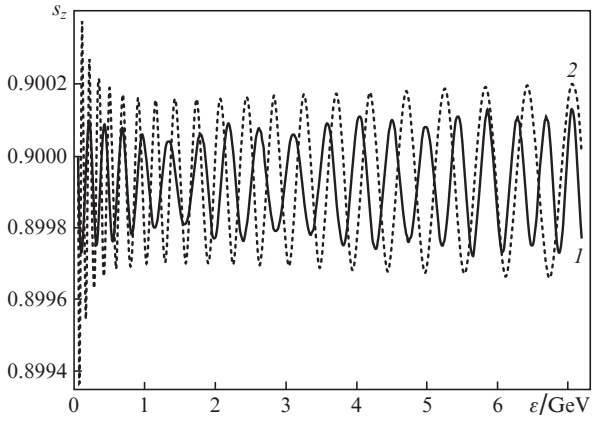

Figure 5. Evolution of the longitudinal spin component of an electron with $\gamma_0 = \gamma_{ph} = 132$ injected at the point $\xi_0 = 3.2$ vs. the electron energy $\varepsilon = \gamma(\tau) mc^2$: the results of numerical calculation for the fields in Figs 3 and 4 (*1*), and calculation according to formula (34) for the average values of the fields acting on the particle during the acceleration process (*2*).

An approximate analytical formula describing the change $\Delta \boldsymbol{s}(t) = \boldsymbol{s}(t) - \boldsymbol{s}_0$ in depolarisation of an electron moving under the action of constant forces (25) can be obtained from (33) with taking into account the equality $s_z^2 + s_\phi^2 + s_r^2 = 1$. Since the variable $\Omega(\tau)$ is much less than unity at $\alpha^2 \gamma_0 \gamma \ll 10^{12}$, the expression for longitudinal component of the spin s_z can be represented in the form of an expansion in the powers of $\Omega(\tau)$. For example, to the accuracy of Ω^2 order terms, we obtain

$$s_z(\tau) = s_{z0} + s_{r0} r_0 \Omega(\tau) - \frac{s_{z0} r_0^2 \Omega^2(\tau)}{2} + O(\Omega^3(\tau)). \qquad (37)$$

This relation results in the following expression for the depolarisation envelope depending on $\gamma(t) = \gamma_0 + E_{ac}\tau$:

$$|\Delta \boldsymbol{s}(\tau)|_{env} = a_m r_0 \sqrt{1 - s_{\phi 0}^2}\, [\alpha^2 \gamma_0 (\gamma_0 + E_{ac}\tau)]^{1/4}. \qquad (38)$$

This equation shows that the depolarisation amplitude is directly proportional to the initial radial displacement r_0 of the electron, and, at the end of acceleration when $\tau \gg \gamma_0 / E_{ac}$, the depolarisation of electrons with equal γ_0 and r_0 becomes the smaller the lesser is the parameter $\alpha^2 E_{ac}$.

A series of calculations has been performed for two values of the electron injection energy. Figure 6 displays the depolarisation envelopes for an electron with the initial energy of 67.5 MeV, which corresponds to $\gamma_0 = \gamma_{ph} = 132$, for its different starting positions r_0 and phases ξ_0, while Fig. 7 shows the depolarisation envelopes for an electron with the initial energy of 10.2 GeV at the same phases and radial positions of the injected electron. The increase in the depolarisation of the electron as a function of its initial offset r_0 with respect to the acceleration channel axis, which is clearly visible when comparing curves (*1*) and (*5*) in Figs 6 and 7, confirms the validity of the approximate analytical relation (38) for the average forces acting throughout the entire length of electron acceleration.

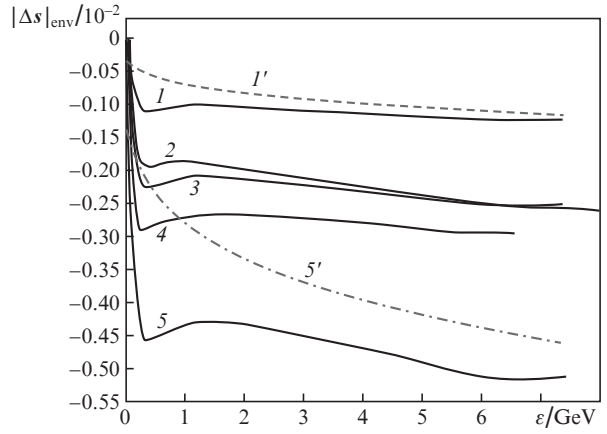

Figure 6. Envelope of the electron depolarisation at the initial energy $\varepsilon_0 = 67.5$ MeV vs. the electron energy $\varepsilon = \gamma(\tau)mc^2$ with $r_0 = 0.125$, $\xi_0 = 3.2$ (*1*), $r_0 = 0.25$, $\xi_0 = 3.0$ (*2*), $r_0 = 0.25$, $\xi_0 = 3.2$ (*3*), $r_0 = 0.25$, $\xi_0 = 3.4$ (*4*) and $r_0 = 0.5$, $\xi_0 = 3.2$ (*5*). Curves (*1′*) and (*5′*) are the calculation according to formula (38) for the parameters corresponding to curves (*1*) and (*5*), respectively.

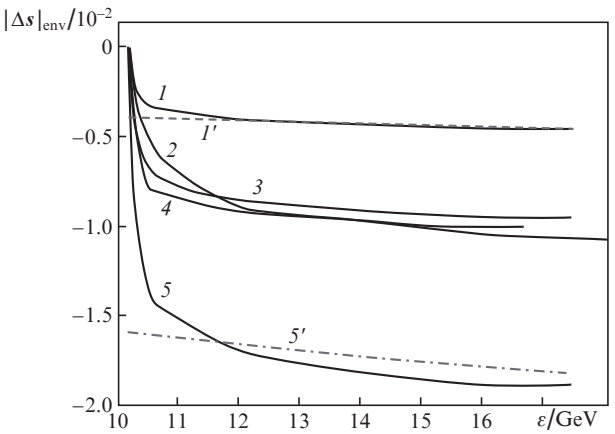

Figure 7. Same as in Fig. 6, but for $\varepsilon_0 = 10.2$ GeV.

Of particular interest is the ultimate value of the electron depolarisation with different injection phases ξ_0. The data in Figs 3 and 4 indicate that the maximal accelerating force acts on the electron with $\xi_0 = 3.0$, and the maximal focusing force acts on the electron with $\xi_0 = 3.4$. As a consequence, the minimal depolarisation value (at the same initial radial offset r_0) is ultimately attained for an electron with $\xi_0 = 3.2$, which is confirmed by the simulation results represented in Figs 6 and 7 [see the curves (*2–4*)].

4. Conclusions

A model that has been developed and tested in the frame of this work has allowed us to study the spin precession dynamics of an electron accelerated by a wake-field wave, generated in the plasma channel by a high-power femtosecond laser pulse, as function of the electron's initial energy and injection phase. It is shown that the electron depolarisation value is directly proportional to the distance between its position in the course of injection and the plasma channel axis; the minimal depolarisation is attained when electrons are injected in the vicinity of the accelerating force's maximum, with a velocity equal to the phase velocity of the wake wave. This model can also be used to study the polarisation dynamics of electron bunches provided that the number N_e of the bunch particles is relatively small: $N_e \ll N_0(c/\omega_{p0})^3$ [8, 14, 18]. Under this condition, the field of the accelerated electron bunch weakly affects the structure of the wake wave generated by a laser pulse (this limitation on the number of accelerated electrons amounts to $N_e \ll 5\times10^8$ for the electron plasma density of $N_0 = 10^{17}$ cm^{-3} discussed in this work).

Acknowledgements. This work wassupported by the Russian Science Foundation (Project No. 14-50-00124).

References

1. Moortgat-Pick G., Abe T., Alexander G., et al. *Phys. Rep*., **460**, 131 (2008).
2. Ali Bagneid A. *Int. J. Mod. Phys. A*, **30**, 1550075 (2015).
3. Shatunov Yu.M. *Puchki polyarizovannykh chastits v uskoritelyakh i nakopitelyakh* (Bunches of Polarised Particles in Accelerators and Storage Rings) (Novosibirsk: Izd-vo SB RAS, 2015).
4. Mane S.R., Shatunov Yu.M., Yokoya K. *J. Phys. G: Nucl. Part. Phys*., **31**, 151 (2005).
5. Tajima T., Dawson J.M. *Phys. Rev. Lett*., **43**, 267 (1979).
6. Modena A., Najmudin Z., Dangor A.E., et al. *Nature (London)*, **377**, 606 (1995).
7. Leemans W.P., Gonsalves A.J., Mao H.-S., et al. *Phys. Rev. Lett*., **113**, 245002 (2014).
8. Andreev N.E., Kuznetsov S.V. *IEEE Trans. Plasma Sci*., **36**, 1765 (2008).
9. Andreev N.E., Chizhonkov E.V., Gorbunov L.M. *Russ. J. Numer. Anal. Math. Modelling*, **13** (1), 1 (1998).
10. Andreev N.E., Gorbunov L.M., Kirsanov V.I., Nakajima K., Ogata K. *Phys. Plasmas*, **4**, 1145 (1997).
11. Mora P., Antensen T.M. *Phys. Plasmas*, **4**, 217 (1997).
12. Andreev N.E., Nishida Y., Yugami N. *Phys. Rev. E*, **65**, 056407 (2002).
13. Sprangle P., Esarey E., Ting A. *Phys. Rev. Lett*., **64**, 2011 (1990).
14. Andreev N.E., Kuznetsov S.V., Pogorelsky I.V. *Phys. Rev. Spec. Top. Accel. Beams*, **3**, 021301 (2000).
15. Bargmann V., Michel L., Telegdi V.L. *Phys. Rev. Lett*., **2**, 435 (1959).
16. Glinec Y., Faure J., Lifschitz A., Vieira J.M. *Europhys. Lett*., **81**, 64001 (2008).
17. Vieira J., Huang C.-K., Mori W.B., Silva L.O. *Phys. Rev. Spec. Top. Accel. Beams*, **14**, 071303 (2011).
18. Ferrario M., Katsouleas T.C., Serafini L., et al. *IEEE Trans. Plasma Sci*., **28**, 1152 (2000).